analytical chemistry

ARTICLE

pubs.acs.org/ac

In Situ Biosensing with a Surface Plasmon Resonance Fiber Grating Aptasensor

Yanina Shevchenko,[†] Tariq J. Francis,[‡] David A. D. Blair,[‡] Ryan Walsh,[‡] Maria C. DeRosa,[*,‡] and Jacques Albert[*,†]

[†]Department of Electronics, Carleton University, 1125 Colonel By Drive, Ottawa, K1S 5B6, Canada

[‡]Department of Chemistry, Carleton University, 1125 Colonel By Drive, Ottawa, K1S 5B6, Canada

Supporting Information

ABSTRACT:

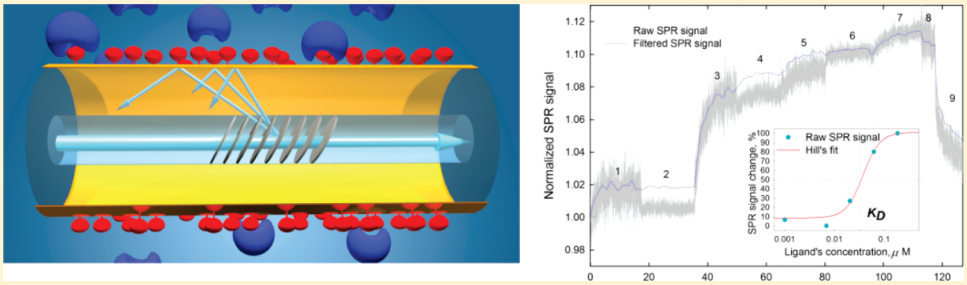

Surface plasmon resonance (SPR) biosensors prepared using optical fibers can be used as a cost-effective and relatively simple-to-implement alternative to well established biosensor platforms for monitoring biomolecular interactions in situ or possibly in vivo. The fiber biosensor presented in this study utilizes an in-fiber tilted Bragg grating to excite the SPR on the surface of the sensor over a large range of external medium refractive indices, with minimal cross-sensitivity to temperature and without compromising the structural integrity of the fiber. The label-free biorecognition scheme used demonstrates that the sensor relies on the functionalization of the gold-coated fiber with aptamers, synthetic DNA sequences that bind with high specificity to a given target. In addition to monitoring the functionalization of the fiber by the aptamers in real-time, the results also show how the fiber biosensor can detect the presence of the aptamer's target, in various concentrations of thrombin in buffer and serum solutions. The findings also show how the SPR biosensor can be used to evaluate the dissociation constant (K_d), as the binding constant agrees with values already reported in the literature.

The rapid and sensitive detection of analytes at low concentrations is paramount in many fields, such as medicine, environmental monitoring, and food safety. Fiber sensors are an appealing solution to this problem because the sensing platform is compact and cost-effective (low cost equipment), and it is possible to collect measurements in situ and remotely. However, the performance of fiber sensors can be compromised by several issues associated with the design of the transducing mechanism and with difficulties arising from the need to modify the fiber geometry. In most fiber biosensors, light guided in the core must be exposed to the external medium in order to perform measurements. This is typically done by removing all or part of the cladding (via etching or side polishing) or tapering down the fiber to allow core guided light to escape into the cladding.[1−3] Another approach consists of the use of a long period grating (LPG) to couple core guided light to cladding guided light.[4] While several fiber-based biosensing platforms have been proposed along these lines, they have not yet been able to replace or compete for real-life applications with other biosensing platforms, such as those relying on planar optical, piezo-electric, or electronic transducing elements. The main reason for this is that all these approaches present practical difficulties that can be overcome in laboratory settings but not in actual use. For instance, the need to etch, taper, or side-polish optical fibers makes them very fragile and requires protective packaging for their use. Also, the cladding removal process must be controlled accurately for each sensor device (with a precision of the order of μm of glass thickness removal). These two factors would increase the cost per sensor to prohibitively high levels in biosensing applications. LPG-based sensors do not suffer from these issues, but their large sensitivity comes with a price: a large cross-sensitivity to everything (especially temperature[5,6]). As a result, while LPG sensors have been around in the literature for as long as Fiber Bragg Grating (FBG) sensors (1994 vs 1989), they have never found widespread use (for any application) while FBGs are now widely deployed in structural engineering[7] and for oil and gas applications.[8] Finally, in the specific case of fiber-based surface plasmon resonance (SPR) sensing, apart from the approaches

Received: April 22, 2011
Accepted: August 4, 2011
Published: August 04, 2011

mentioned above and their limitations for general fiber biosensors, cladding-removed multimode fibers have been the most successful devices so far.[3] In fact, recent results showing high sensitivity fiber SPR biosensing[3,9] are still based on the concept originally demonstrated by Yee et al. in 1993.[10] The issue with these multimode sensors is that the polarization state and the distribution of the light among all possible cladding modes must be controlled and maintained with a high degree of precision. This requires strictly controlled launch conditions at the input of the fiber, short fiber lengths without sharp bends, and the absence of fiber motion during experiments (or between experiments if comparative measurements are required).

The sensor presented here avoids all of the above issues using a single-mode tilted Fiber Bragg Grating (TFBG). It combines a number of technologies to create a simple and robust platform that has been successfully applied to a full range of target—analyte interactions.[11] The sensing mechanism used in this study relies on SPR, which is a unique electro-magnetic phenomenon occurring at the interface between materials with opposite dielectric constants.[12] It allows for the detection of material changes occurring at the nanometer level in layers adjacent to this interface. As a result, SPR has been successfully applied for the characterization of various biomolecular reactions and their dynamics.[13] SPR platforms traditionally employed in biosensing use the total internal reflection of light on the base of a high refractive index prism to excite Plasmon waves, as in the so-called "Kretschmann" configuration.[14] Although the prism-based SPR platform has a high sensitivity, it is rather costly, bulky, and limited because it can only be applied in a laboratory environment. Thus, SPR sensing platforms utilizing an optical fiber as a transducing element have gained considerable attention since it allows for the sensor design to be very compact and cost-effective. Another advantage is gained if a single-mode fiber is used, making it possible to operate remotely over large distances because there is no issue with the modal distribution of the guided light that reaches the sensor element. However, compared to the commonly used prism-based SPR configuration, the implementation of SPR on the surface of an optical fiber is more challenging because light propagating in a fiber has to be first "phase-matched" and polarized perpendicular to the metal surface to allow coupling to the surface Plasmon waves. The latter is especially challenging because of the cylindrical symmetry of the fiber. Another issue is the spectral width of the SPR resonance: in all fiber-SPR approaches developed so far (and in fact also in most bulk optic SPR instruments), the SPR resonances have had widths of the order of tens of nm. Since the spectral resolution (minimum detectable wavelength shift) required to achieve low concentration biochemical sensing is of the order of pm,[1,9] such wide resonances hinder reproducibility and accuracy (a commonly used figure of merit for optical resonant sensors is the spectral sensitivity divided by the spectral width of the resonance).[1]

The sensor we propose here uses ordinary single mode fiber, does not require physical modification of the fiber, provides a mechanism to eliminate cross-sensitivities (including temperature), and automatically generates a dense comb-like spectrum of narrowband (0.1 nm wide) SPR active resonances of the optimum polarization.[15] Those resonances that are phase matched to the SPR have sensitivities between 500 and 1000 nm/RIU (RIU = refractive index units). Unlike FBG or LPG approaches, a single sensor design can be used for media with refractive indices ranging from 1.25 to 1.4, also contributing to the low cost per sensor as the same design can be used in multiple applications.

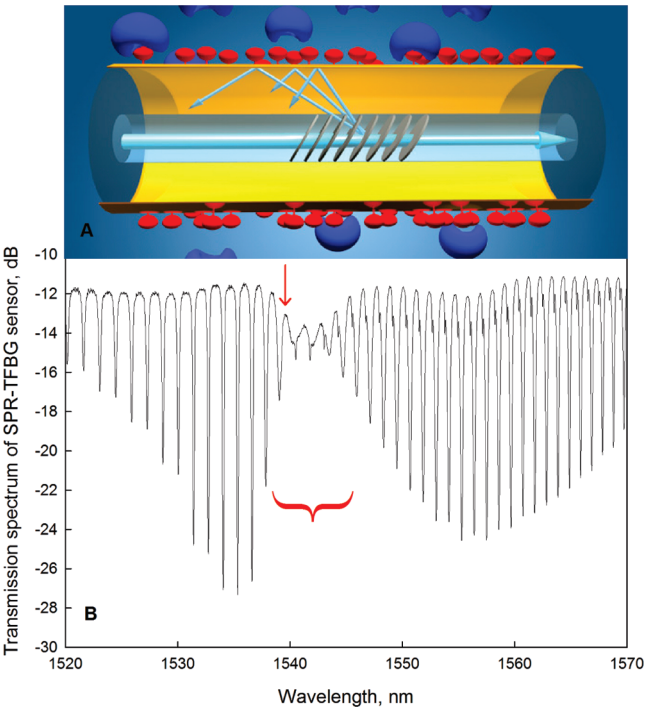

Figure 1. (A) 3D illustration of the presented SPR-TFBG biosensor: a standard optical fiber with a TFBG imprinted in its core coupling light to the SPR. A monolayer of thrombin aptamer probes (shown in red) immobilized on the gold coating interacts with their cognate thrombin protein targets (shown in blue). (B) Sensor's response measured in the aptamer solution, SPR-coupled part is shown with red brackets. The red arrow indicates the most sensitive SPR-coupled cladding resonance.

These features of the TFBG-SPR sensor are obtained because the grating is imprinted in the fiber core at a certain angle relative to the longitudinal axis of the fiber. This results in the excitation of tens of claddings modes (Figure 1A), each at a unique well-defined wavelength, over a relatively modest spectral window (approximately 100 nm). Some of the excited cladding modes can couple to a SPR wave on the surface of the fiber if the SPR phase matching condition is satisfied, as determined by the refractive index of the medium immediately adjacent to the fiber surface.[15] Furthermore, the tilt plane of the TFBG breaks the internal cylindrical symmetry and allows the user to select the dominant polarization of the excited cladding modes for optimum SPR coupling.[16] We use an unmodified and inexpensive standard telecommunication single mode fiber (CORNING SMF-28) in these experiments, making the sensor very robust and simple to manufacture. TFBGs are fabricated with the same tools and techniques as FBGs, and these are now mass produced at very low cost per sensor in highly automated factories for use by the structural sensing community.[17] Besides being robust, the single mode fiber has no issues with the modal distribution of the guided light that reaches the sensor element: in multimode sensors, changes in modal distribution impact the shape of the SPR resonance and our ability to track it accurately over small wavelength shifts. Furthermore, the single mode fiber's transmission loss is 0.17 dB/km[18] (or equivalently, less than 4% of power loss per km) while the dynamic range for measuring the transmission of in-fiber devices with widely available telecommunication

instrumentation (since we are using ordinary telecommunication fiber in its normal wavelength range) is well over 40 dB (or 99.99%). Such low transmission losses could allow for remote operation over large distances (up to multikm distances).

A final, unique advantage associated with the use of TFBGs is the elimination of the effect of temperature cross-sensitivity from the sensor readings. In other kinds of SPR sensors, the well-known cross-sensitivity of the SPR coupling condition on temperature requires stringent temperature control during experiments and the presence of a temperature sensor or second sensing element. This problem essentially negates the possibility of remote, in situ sensing that fiber devices should be able to achieve. Although our metal-coated TFBGs are also sensitive to temperature variations, it is possible to eliminate this effect during the processing of the experimental data (even in real time). This is due to the invariance of the overall transmission spectrum of the TFBG to the temperature and the presence of a core-mode spectral resonance whose wavelength only depends on the temperature. Also, if needed, the core mode resonance can be used as a high accuracy local thermometer (with 0.1 °C precision).[19]

Having a wide operating range, a relatively high wavelength shift sensitivity of 400−1000 nm/RIU, depending on the resonance used,[20] and a very simple fabrication method has allowed this sensor platform to be successfully applied for chemical sensing and real-time in situ monitoring of polyelectrolyte multilayer formation.[14] The material presented here deals with the first comprehensive study of this novel sensor technology toward biosensing.

As molecular recognition is the cornerstone of biosensing, an essential component to any biosensor is the specific molecular recognition probe that can target the analyte of interest. While antibodies have been the gold standard for molecular recognition probes for several decades, the relatively new technology of aptamers is emerging as a more robust and cost-effective alternative. Aptamers are short oligonucleotide sequences that can be synthesized to bind with a strong affinity and specificity to a given molecular target.[21,22] Aptamers have already been successfully applied as molecular recognition probes for a variety of sensor techniques such as electrochemical,[23,24] piezoelectric,[25,26] and optical sensors.[22,27,28] Prism-based SPR sensors have also been previously reported to use aptamers.[26,29,30] In the field of biosensing, one of the most promising advantages associated with the use of aptamers is the possibility of synthesizing aptamers that bind to a wide range of targets including drugs,[31] proteins,[32] or even supramolecular complexes such as viruses or bacteria.[33,34] Recently, an aptamer-modified biosensor[9] using a pre-existing and partially automated SPR sensor platform was implemented in an etched multimode fiber.[10] Taking into account growing interest toward aptamers as highly modifiable and versatile biorecognition elements and the advantages of fiber-based SPR sensors, we were interested in studying the effectiveness of an aptamer-based SPR sensor implemented with our TFBG, standard single-mode fiber platform (See Figure 1). In this way, we sought to avoid the drawbacks of the use of a modified, multimode fiber, while preserving the ease of use, sensitivity, and selectivity of an aptamer−fiber system. Our experimental results indicate that our sensor can be used for the real-time monitoring of both the self-assembly of aptamers on the surface of a gold-coated fiber as well as for detection of protein molecules at various concentrations in solutions including serum. The dissociation constant (K_d) of the target bound to the aptamer−sensor surface was determined and was found to be comparable to that found in solution studies.

EXPERIMENTAL SECTION

Fabrication of the TFBG-SPR Sensor. As reported earlier,[15,16,35] the SPR-TFBG sensor was manufactured using a standard single-mode fiber (Corning SMF-28) with a TFBG inscribed in the fiber's core and gold coating deposited on the surface of the fiber's cladding. TFBG was manufactured using the phase-mask technique: it required shining of UV light at 248 nm onto the surface of a bare fiber that was previously saturated with hydrogen. The grating's planes were written with a certain tilt relatively to the longitudinal axis of the fiber (Figure 1A). Tilt of the grating is an important parameter that can be used to choose which set of cladding modes is going to be excited. As a result, it makes it possible to adjust the operating range of the sensor in order to optimize the response for certain refractive indices. Here, the gratings had a tilt of 10°, which allowed them to operate in aqueous solutions with refractive indices around 1.31−1.34.

A thin gold coating was deposited on the surface of the fiber after the gratings were inscribed. Deposition was conducted in a vacuum sputtering chamber and required two consecutive runs with the fiber being rotated by 180° between depositions to ensure a more or less uniform coating around the circumference of the fiber. Thickness of the gold layer was optimized to have the strongest SPR effect and was selected to be 50 nm for these experiments.

Experimental Setup, Optical Configuration. The experimental setup required the sensor to operate in the transmission regime. During the experiments, the sensors had to be fixed in a 7.5 cm by 2 cm plastic cell designed specifically for the biosensing tests. While each individual sensor was fixed in the platform with help of UV-sensitive adhesive, the sensing element (0.5 cm in length) was immersed in a carved out indentation (45 mm by 5 mm), which was then covered by a glass slide to avoid evaporation of fluids during the experiments. Immersion of the sensor was conducted at the beginning of each test using a pipet; on average, 600 μL of fluid was added.

Sensors were interrogated using an Optical Sensing Analyzer (model Si720 from Micron Optics). Light over the 1520−1570 nm range was linearly polarized using Polarization Controller from JDS Uniphase. Before each experiment, the orientation of the polarization was adjusted to maximize coupling of the cladding modes to the SPR to ensure the strongest contrast between SPR-coupled and non-SPR modes. The measurement resolution was set at 0.0025 nm, and measurements were recorded each 0.8 s. A schematic of the used optical setup can be found in the Supporting Information (Figure S1).

Analysis of the Experimental Data. Figure 1B provides an example of the typical transmission spectrum obtained with the SPR-TFBG sensor while being immersed in the aptamer solution, making it possible to excite the SPR. The red bracket in Figure 1B denotes the portion of the SPR-modified spectrum. The analysis presented in this paper is based on tracking the changes in the SPR-modified portion of the spectrum, more particularly, tracking of the most sensitive SPR coupled cladding resonance. This resonance occurs on the left from the narrowest part of the SPR-coupled region, as indicated by the red arrow in Figure 1B. The power level of the maximum of that resonance was taken into account during evaluation of the SPR signal change.

Evaluation of the SPR signal change based on this method, where the absolute value of the position of only one resonance is considered, was applied for analysis of the data where the refractive index change was anticipated to be relatively small. Such experiments included simple one-step tests with a certain chemical reaction taking place on the surface of the sensor, such as self-assembly of aptamers or binding of target molecules to the aptamers. However, experiments, where a larger refractive index change occurred, required a different approach that would ensure consistency between the data sets obtained during different parts of the experiment. Such experiments, where the sensor was immersed in several solutions with different refractive indices, would be impossible to analyze taking into account the same SPR-coupled resonance because different solutions would result in different resonances being identified as the most sensitive. Thus, the analysis of such tests was based on tracking of the normalized amplitude value of that resonance. Such normalization ensured that the SPR changes happening in different solutions and affecting different resonances with different amplitudes could be compatible and comparable. Data analysis based on normalized value of the resonance's amplitude was applied for the K_d evaluation (see below). All experimental data was smoothed using a 400-term LOESS filter.[36]

Aptamer Sequences, Buffers, Serum, Thrombin Protein, and Water. All buffer solutions were prepared using doubly deionized water from a Milli-Q water system (ThermoFisher). All DNA phosphoramidites and modifiers were purchased from Glen Research. Bovine serum and bovine serum albumin were purchased from Sigma Aldrich. Bovine serum solution for testing was prepared as a solution of 50% serum/50% Tris buffer (50 mM Tris, 1 mM $MgCl_2$, 140 mM NaCl, 5 mM KCl). The thiolated thrombin aptamer, DNA sequence HS-$(CH_2)_6$-5′-GGT TGG TGT GGT TGG-3′ (herein called thrombin aptamer), was synthesized on a MerMADE 6 DNA synthesizer (Bioautomation Corporation). The sequence purification was conducted using Clarity QSP Cartridges (Phenomenex). The DNA was dissolved in "DNA buffer" (5 mM phosphate, 100 mM $MgCl_2$, 50 mM NaCl). DNA sequences were confirmed by ESI-MS, and the Ellman's test[37] was conducted to test for presence of the 5′ Thiol group prior to binding.

Human α-thrombin protein was purchased from Haematologic Technologies Inc. The protein was aliquoted as needed and dissolved in "protein buffer" (50 mM Tris, 1 mM $MgCl_2$, 140 mM NaCl, 5 mM KCl).

The sequences used for the confocal microscopy experiments were purchased from Alpha DNA (Montreal). The thrombin aptamer sequences possessed the 5′-thiol′C6 modifier, as well as a Cyanine 3 (Cy3) dye modifier at the 3′ end, making the overall sequence 5′-HS-$(CH_2)_6$-GGT TGG TGT GGT TGG-Cy3-3′ (herein called Cy3 DNA).

Immobilization of the Thrombin Aptamer. Prior to the immobilization of the thrombin aptamer on the surface of the sensor, the sensors were washed with ethanol and then with Milli-Q water. After the cleaning step, DNA functionalization was conducted by filling out the carved indentation with the aptamer solution of the desired concentration. Transmission spectra were collected automatically every 0.8 s during the entire experiment. Aptamer deposition times and concentrations varied between tests. After the aptamer adsorption step was complete, the sensor was rinsed with DNA buffer several times before the protein solution was added.

Binding of the Thrombin Protein to the Thrombin Aptamer. Thrombin solutions were prepared to a desired concentration using human α-thrombin and protein buffer. The solutions were used to fill the cut out indentation of the platform. The duration of soaking in the thrombin solution varied between 20 min and 2 h depending on the experiment. After immersion in the protein solution, the sensor was washed with protein buffer for several minutes to prepare for the next step.

Confocal Microscope Imaging. Confocal microscope imaging combined with fluorescent labeling was used to evaluate and confirm the self-assembly of the aptamer on the surface of the gold coating of the sensors. All confocal microscopy images were collected on a Zeiss LSM510 with a Plan-Acochromat 63×/1.4 Oil Dic objective with LP950 filter, with an excitation wavelength of 550 nm and an emission wavelength of 570 nm.

Before running the experiment, the sensors were prepared by rinsing them with anhydrous ethanol and then with DNA buffer. Cy3 DNA was dissolved in DNA buffer to make a 45 μM solution. Sensors were then immersed in the aptamer solution for 20 h, rinsed thoroughly, and later imaged while mounted on microscope slides in a solution of 50% glycerol in water and covered with 1.7 μm thick cover slides.

Atomic Force Microscope (AFM) Imaging. AFM imaging was conducted in order to evaluate the surface of the sensor after binding to thrombin protein. All AFM images were collected on an Ntegra system using a SFC050LNTF AFM Head on an inverted microscope (Olympus IX71). (See Supporting Information for details regarding AFM tools.) Before imaging, gold-coated fibers were immersed in a 25 μM solution of thiolated thrombin aptamer for a period of 4 h. The fiber was then rinsed with DNA buffer and immersed in a 30 μM solution of α-thrombin in protein buffer for approximately 12 h. After immersion, the fibers were rinsed with Milli-Q water and dried in air before imaging. All samples were collected in air on the dry samples.

RESULTS AND DISCUSSION

Monitoring of Thrombin−Aptamer Self-Assembly. Results of the experiments that involved soaking of the sensor in the aptamer solutions of varying concentrations are shown in Figure 2. Raw SPR data is shown in the sensorgram in Figure 2A along with the filtered signal in order to illustrate a difference between both types of signals. As it can be seen, the signals obtained in the solutions with aptamers showed a considerable increase over the first 6 to 8 min of soaking (Figure 2A) and then showed a much slower change, suggesting that initial binding of the aptamer to the surface occurs quickly. Moreover, the signal obtained from soaking in the DNA buffer was significantly lower than the signal obtained in the aptamer solutions. Doubling the aptamer concentration from 10 to 20 μM did not lead to a doubling of the signal, suggesting that 20 μM aptamer is concentrated enough to saturate the surface for our experiments.

Attachment of the aptamers was verified using confocal fluorescent imaging (Figure 3A). DNA modified with the fluorescent Cy3 dye was immobilized on the surface of the sensor and was imaged after unbound aptamers were rinsed away during the washing step. A fluorescent signal coming from the fiber surface can clearly be seen in the case of the Cy3 DNA modified surfaces. As a control, a bare sensor immersed in a solution of free Cy3 dye showed no fluorescence (see Supporting Information, Figure S3 A-B). These results confirm the immobilization of the modified thrombin aptamer sequence on the surface of the fiber.

Detection of the Thrombin Target. Thrombin is a multifunctional protein that helps regulate many physiological processes

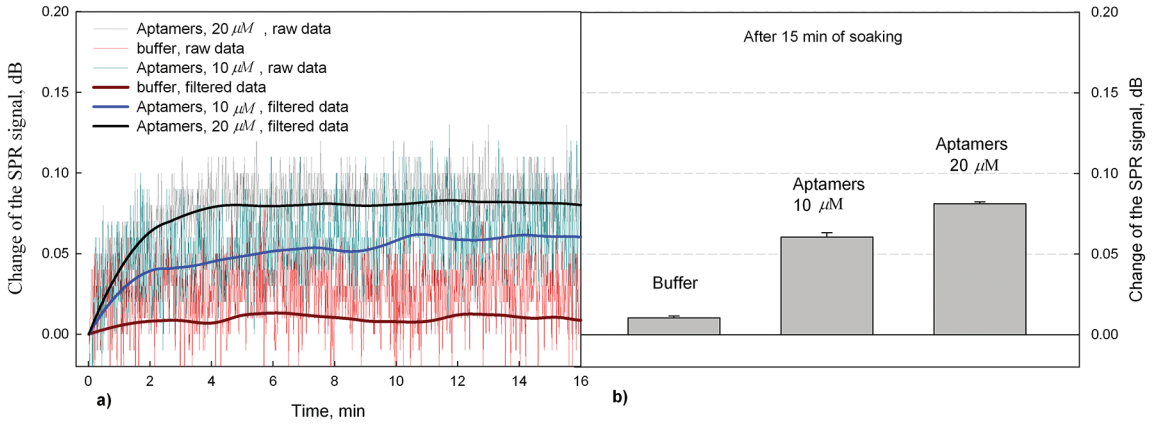

Figure 2. (A) Real-time SPR signal changes over the first 15 min of aptamer self-assembly versus soaking in the DNA buffer and Milli-Q water; raw SPR signal is shown along with filtered data. (B) Bar diagram illustrating difference in SPR signals after the first 15 min of soaking in solutions.

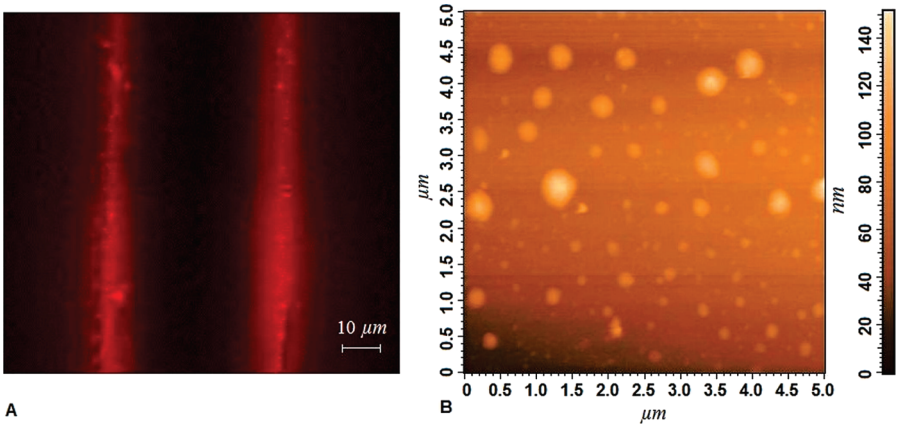

Figure 3. (A) Confocal microscope image of an optical fiber immersed in a 45 μM Cy3- and thiol-modified DNA solution for 20 h; 11% laser strength, detector pinhole width of 55 μm, and 63× magnification were applied. (B) AFM image of sensor's surface after attachment of the thrombin (tapping mode, measured in air on the dry sample).

including the coagulation of blood. During a coagulation reaction, dynamically changing thrombin concentrations from 1 nM to greater than 500 nM have been observed.[38] A sensor able to detect thrombin at these concentrations, in situ and in real-time, could provide valuable insight into conditions associated with abnormal thrombin generation. Moreover, the thrombin aptamer is one of the best characterized and widely studied protein-binding aptamers. Therefore, using thrombin detection as a test case for our SPR-TFBG aptasensor should serve as an indication that this system could be used to detect and monitor other proteins found in human plasma or blood that could be of interest to the science community.

Results of the immersion of the aptamer-functionalized sensor into the thrombin solutions are shown in the Figures 3B and 4. Figure 4A indicates that, similarly to soaking in DNA solution, the SPR signal changes rapidly within the first 10 min of immersion and then stabilizes. In addition to the signal comparison with protein buffer, several control solutions were also examined. BSA is typically used as a control for thrombin aptamer studies;[39] however, it is much larger than thrombin which can lead to some nonspecific binding (67 kDa compared to thrombin's 37 kDa). Pepsin, which is comparable in size to thrombin (35 kDa) and should have no affinity for the thrombin aptamer, was also examined in order to gain a better perspective regarding nonspecific binding. Comparison of the thrombin data against that generated by soaking in the BSA, pepsin, and buffer solutions indicates that selective detection of target molecules at concentrations that are as low as 0.1 μM is possible. A difference in signals can be detected in as little as 10 min (Figure 4A). However, after 100 min, the signals have stabilized and show the greatest discrimination between specific and nonspecific signals (Figure 4B). As real samples will undoubtedly contain interferences at concentrations higher than those tested in our control experiments, evaluation of the sensor's response in a more complex solution such as serum was also attempted as shown in the bar diagram, Figure 4B. The 50% bovine serum solution used for these experiments has a nonspecific protein concentration of 30 mg/mL. The results for soaking in serum and serum mixed with thrombin (5 μM or 0.18 mg/mL) show that, despite a strong nonspecific signal increase in the presence of serum, the attachment of thrombin at a concentration more than 2 orders of magnitude lower than the interfering agents can still be detected. The absolute SPR signal difference between the 50% serum solution and the 5 μM thrombin−serum solution (approximately 0.07 dB) is very similar to the difference between buffer and 5 μM thrombin−buffer solution (0.074 dB) Thus, the

dx.doi.org/10.1021/ac201641n |*Anal. Chem.* 2011, 83, 7027–7034

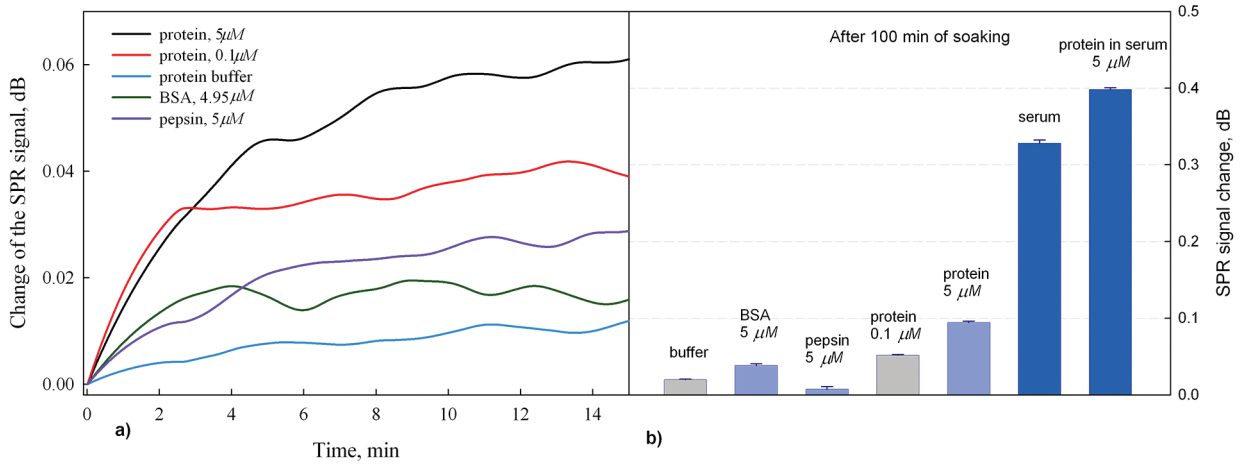

Figure 4. (A) Real-time SPR response measured during the first 15 min of soaking in 0.1 and 5 μM thrombin solutions versus soaking in 5 μM BSA, 5 μM pepsin, and protein buffer. (B) Bar diagram comparing SPR response obtained in serum and protein solutions after soaking for 100 min.

specific thrombin−aptamer interactions can be effectively detected, even in complex media. Errors found as a standard deviation describe the uncertainty between the filtered signal and a linear fit where the signal became saturated and leveled off.

The attachment of protein was confirmed by imaging the sensor's surface using AFM (Figure 3B). AFM reveals that the scanned sensor's surface has many new structural features with sizes at the μm and subμm scale that are not present on the aptamer modified surface alone (see Supporting Information for 3D AFM images, Figure 4S A−C). It is anticipated that a molecule of thrombin protein has a dimension of 4.5 × 4.5 × 5 nm,[40] which is much smaller than the observed features. A possible explanation of observed features could be that the protein molecules formed clusters in the solution before or during the interaction with aptamer molecules. In the latter case, formation of protein clusters on the surface of the sensor could be a result of the uneven distribution of aptamer molecules on the surface of the sensor, a finding that has been previously reported.[34]

Even though the thrombin molecules did not form a uniform layer on the surface of the sensor, measured SPR signal changes should be proportional to the overall protein amount adsorbed to the surface of the grating. The SPR is excited over the full length of the grating, which is 1 cm; therefore, the observed SPR response was averaged over the length of the TFBG that was used to excite the SPR.

Sensor Characterization and K_d Analysis. Signal to noise ratio (SNR) and limit of detection (LOD) are important parameters for the characterization of sensor performance. The SNR for our system varied from 2.11 to 194.51 for the experiments with thrombin (Figure 4B) and from 8.58 to 36.97 for experiments with aptamers (Figure 3B). The limit of detection of thrombin (LOD) was calculated as 3 times the noise level[41] and was found to be 22.6 nM. This compares well to the 2 nM LOD reported by Pollet et al.[9] for another fiber SPR sensor.

The dissociation constant (K_d) is a widely used parameter applied to characterize binding strength between two interacting molecules. The motivation behind using a fiber biosensor for determining K_d constants stems from the interest in developing a portable sensor platform that can be applied to the in situ measurement of biomolecular kinetic interactions without perturbing the surrounding environment.

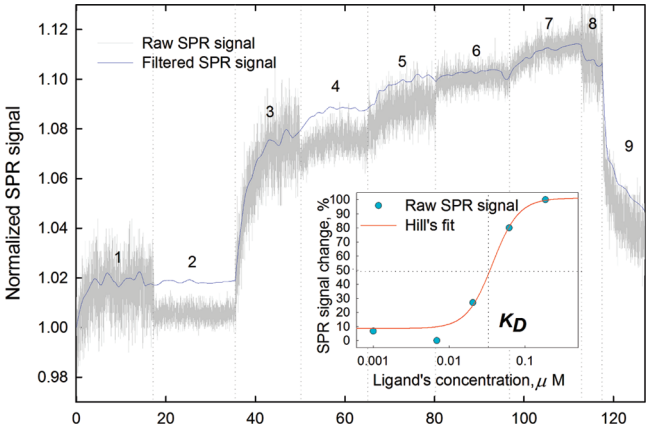

Figure 5. SPR signal change during the K_d- type test ("Ladder" test). Description of each step: (1) Milli-Q water; (2) DNA buffer; (3) aptamers concentration, 20 μM; (4) thrombin concentration, 0.1 μM; (5) thrombin concentration, 0.5 μM; (6) thrombin concentration, 1 μM; (7) thrombin concentration, 5 μM; (8) protein buffer; (9) regeneration in 0.2 M of Na_2CO_3. Inset: Evaluation of the K_d constant using relation between ligand's concentration and SPR signal. The data set was normalized to the maximum of the SPR signal and was fitted using Hill's equation.[45] (See Supporting Information for information regarding the fitted model and K_d experiment's data.)

The dissociation constant (K_d) for the thrombin aptamer has been reported earlier, based on studies,[42,43] to be between 20 and 200 nM. However, it is well-known that the functionalization of aptamers to surfaces may alter the binding characteristics of the system.[44] Therefore, the characteristics of the immobilized aptamers and their effect on the binding dynamics had to be assessed.

Evaluation of the K_d constant was performed using an analyte "Ladder" test. Initially, the sensor was functionalized with the aptamer followed by its immersion in successive solutions of increasing concentrations of the target. Figure 5 shows the results of one ladder experiment where the sensor was immersed in a set of solutions with thrombin concentration increasing from 0.1 to 5 μM. The SPR signal (raw and smoothed data) was obtained by normalizing the amplitude of the most sensitive SPR-coupled resonance. Figure 5 illustrates the correlation between increase in

SPR signal and deposition of the aptamer (step 3). This was followed by subsequent soaking of the sensor in solutions of increasing thrombin concentration (steps 4−7). Washing with protein buffer (step 8) did not lead to a dramatic loss of signal, confirming the specific interaction between the protein and the sensor. Removal of the biomolecular layer was achieved by soaking in sodium carbonate (step 9). The inset in Figure 5 illustrates the relationship between normalized SPR signal change and thrombin concentration that was used to determine K_d. It was found that the K_d for the sensor was approximately 40 ± 1 nM, indicating that attachment of the aptamer to the gold surface of the sensor did not significantly affect the binding affinity between the aptamer and thrombin. See Supporting Information, Figure S5, for K_d SPR data and for details regarding the model fit applied to evaluate the K_d constant. This suggests that this method of sensor generation offers the potential for cheap portable alternatives to the bulky expensive systems usually associated with analytical detection methods.

CONCLUSIONS

This study demonstrates, for the first time, how a TFBG-SPR sensor manufactured from an unmodified single mode fiber can be used as a biosensor to detect a biomolecular target at varying concentrations. The results showed that the TFBG-SPR sensor could be successfully applied to biosensing studies making this biosensor platform a strong alternative to the existing biosensing modalities that rely on optical and nonoptical transducing elements. More specifically, this system can be used for the real-time quality control of sensor manufacturing as the self-assembly of the sensor can be monitored. It was reported that aptamers, which were used as the biorecognition element, attach themselves to the surface, providing the same signal observed in the detection of the analyte itself. This system provided a robust detection of thrombin in buffer and more complex solutions such as serum. The signal difference between specific and nonspecific interactions remained the same regardless of the solution, which suggests several possibilities for future work in complex environments.

The findings confirmed that the biosensor can be applied for traditional real-time characterization of biorecognition element−target interactions, as well as for a multistep analysis to determine the K_d constant. The value of K_d was found to be well within the range of values already reported in the literature. These findings together suggest that this sort of sensor platform could be used for the in situ characterization of biochemical reactions which makes it a viable alternative to other more costly or bulky well-established analytical tools.

ASSOCIATED CONTENT

Supporting Information. Information about the optical setup, AFM setup, and the K_d study and AFM images. This material is available free of charge via the Internet at http://pubs.acs.org.

AUTHOR INFORMATION

Corresponding Author

*E-mail: jacques_albert@carleton.ca; Tel: +1613-520-2600 x5578. Fax: +1613-520-5708 (J.A.). E-mail: maria_derosa@carleton.ca; Tel: (613) 520-2600 x3844. Fax: (613) 520-3749 (M.C.D.).

ACKNOWLEDGMENT

This work was supported by the Natural Sciences and Engineering Research Council of Canada, Canada Research Chair Program, the Ontario Early Researcher Award, and LxData Inc., Montreal. We would like to thank Dr. Anatoli Ianoul and Graham Galway for assisting with the AFM imaging of the sensor samples. We would also like to acknowledge Anne-Fook Yang, Denise Chabot, and Yasir Sultan from Agriculture Canada for helping us acquire the confocal fluorescent images.

REFERENCES

(1) Fan, X.; White, I. M.; Shopova, S. I.; Zhu, H.; Suter, J. D.; Sun, Y. *Anal. Chim. Acta* **2008**, *620*, 8–26.
(2) Lee, B.; Roh, S.; Park, J. *Opt. Fiber Technol.* **2009**, *15*, 209–221.
(3) Sharma, A. K.; Jha, R.; Gupta, B. D. *IEEE Sens. J.* **2007**, *7*, 1118–1129.
(4) Pilla, P.; Manzillo, P. F.; Malachovska, V.; Buosciolo, A.; Campopiano, S.; Cutolo, A.; Ambrosio, L.; Giordano, M.; Cusano, A. *Opt. Express* **2009**, *17*, 20039–20050.
(5) Kersey, A. D.; Davis, M. A.; Patrick, H. J.; LeBlanc, M.; Koo, K. P.; Askins, C. G.; Punam, M. A.; Friebele, E. J. *J. Lightwave Technol.* **1997**, *15*, 1442–1463.
(6) Mishra, V.; Singh, N.; Tiwari, U.; Kapur, P. *Sens. Actuators, A* **2011**, *167*, 279–290.
(7) Majumder, M.; Gangopadhyay, T. K.; Chakraborty, A. K.; Dasgupta, K.; Bhattacharya, D. K. *Sens. Actuators, A* **2008**, *147*, 150–164.
(8) Zhang, Y.; Li, S.; Yin, Z.; Chen, B.; Cui, H.-L.; Ning, J. *Opt. Eng.* **2006**, *45* (084404), 1–4.
(9) Pollet, J.; Delport, F.; Janssen, K. P. F.; Jans, K.; Maes, G.; Pfeiffer, H.; Wevers, M.; Lammertyn, J. *Biosens. Bioelectron.* **2009**, *25*, 864–86.
(10) Jorgenson, R. C.; Yee, S. S. *Sens. Actuators, B: Chem.* **1993**, *12*, 213–220.
(11) Magius, S.; Laffont, G.; Ferdinand, P.; Carbonnier, B.; Kham, K.; Mekhalif, T.; Millot, M.-C. *Opt. Express* **2008**, *16*, 19049–19062.
(12) Raether, H. *Surface Plasmons on Smooth and Rough Surfaces and on Gratings*; Springer-Verlag: Berlin, Germany, 1988.
(13) Homola, J. *Chem. Rev.* **2008**, *108*, 462–493.
(14) Kretschmann, E.; Raether, H. *Z. Naturforsch.* **1968**, *A 23*, 2135–2136.
(15) Shevchenko, Y. Y.; Albert, J. *Opt. Lett.* **2007**, *32*, 211–213.
(16) Shevchenko, Y.; Chen, C.; Dakka, M. A.; Albert, J. *Opt. Lett.* **2010**, *35*, 637–639.
(17) Albert, J.; Chen, C.; Shevchenko, Y.; Ivanov, A. Tilted grating sensor, PCT (International patent application) WO2008/049187-A1 (publication date May 2, 2008).
(18) Corning, 2010. Corning SMF-28 ULL Optical Fiber with Corning Ultra Low-Loss Technology. http://www.corning.com/WorkArea/showcontent.aspx?id=14357 (accessed on Aprl 15, 2010).
(19) Shao, L. Y.; Shevchenko, Y.; Albert, J. *Opt. Express* **2010**, *18*, 11464–11471.
(20) Caucheteur, C.; Shevchenko, Y.; Shao, L.-Y.; Wuilpart, M.; Albert, J. *Opt. Express* **2011**, *19*, 1656–1664.
(21) Rimmele, M. *ChemBioChem* **2003**, *4*, 963–971.
(22) Cho, E. J.; Lee, J.; Ellington, A. D. *Annu. Rev. Anal. Chem.* **2009**, *2*, 241–264.
(23) Ikebukuro, K.; Kiyohara, C.; Sode, K. *Biosens. Bioelectron.* **2005**, *20*, 2168–2172.
(24) So, H. M.; Won, K.; Kim, Y. H.; Kim, B.-K.; Ryu, B. H.; Na, P. S.; Kim, H.; Lee, J.-O. *J. Am. Chem. Soc.* **2005**, *127*, 11906–11907.
(25) Liss, M.; Petersen, B.; Wolf, H.; Prohaska, E. *Anal. Chem.* **2002**, *74*, 4488–4495.
(26) Tombelli, S.; Minunni, M.; Luzi, E.; Mascini, M. *Bioelectrochemistry* **2005**, *67*, 135–141.
(27) Jhaveri, S. D.; Kirby, R.; Conrad, R.; Maglott, E. J.; Bowser, M.; Kennedy, R. T.; Glick, G.; Ellington, A. D. *J. Am. Chem. Soc.* **2000**, *122*, 2469–2473.

(28) Stojanovic, M. N.; De Prada, P.; Landry, D. W. *J. Am. Chem. Soc.* **2001**, *123*, 4928–4931.
(29) Ostatná, V.; Vaisocherová, H.; Homola, J.; Hianik, T. *Anal. Bioanal. Chem.* **2008**, *391*, 1861–1869.
(30) Wang, J.; Zhou, H. S. *Anal. Chem.* **2008**, *80*, 7174–7178.
(31) Xiao, H.; Edwards, T. E.; Ferre-DèAmare, A. R. *Chem. Biol.* **2008**, *15*, 1125–1137.
(32) Keefe, A. D.; Pai, S.; Ellington, A. *Nat. Rev. Drug Discovery* **2010**, *9*, 537–550.
(33) Bruno, J. G.; Carrillo, M. P.; Phillips, T.; Andrews, C. J. *J. Fluoresc.* **2010**, *20*, 1211–1223.
(34) Jeon, S. H.; Kayhan, B.; Ben-Yedidia, T.; Arnon, R. *J. Biol. Chem.* **2004**, *279*, 48410–48419.
(35) Shevchenko, Y.; Ahamad, N. U.; Ianoul, A.; Albert, J. *Opt. Express* **2010**, *18*, 20409–20421.
(36) Cleveland, W.S. J. *Am. Stat. Assoc.* **1979**, *74*, 829–835.
(37) Ellman, G. L. *Arch. Biochem. Biophys.* **1959**, *82*, 70–77.
(38) Wolberg, A. S. *Blood Rev.* **2007**, *21*, 131–142.
(39) Rahman, M. A.; Son, J. I.; Won, M.; Shim, Y. *Anal. Chem.* **2009**, *81*, 6604–6611.
(40) Bode, W.; Mayr, I.; Baumann, U.; Huber, R.; Stone, S. R.; Hofsteenge, J. *EMBO J.* **1989**, *8*, 3467–3475.
(41) Vial, J.; Jardy, A. *Anal. Chem.* **1999**, *71*, 2672–2677.
(42) Bock, L. C.; Griffin, L. C.; Latham, J. A.; Vermaas, E. H.; Toole, J. J. *Nature* **1992**, *355*, 564–566.
(43) Hamaguchi, N.; Ellington, A.; Stanton, M. *Anal. Biochem.* **2001**, *294*, 126–131.
(44) Jing, M.; Bowser, M. T. *Anal. Chim. Acta* **2011**, *686*, 9–18.
(45) Goutelle, S.; Maurin, M.; Rougier, F.; Barbaut, X.; Bourguignon, L.; Ducher, M.; Maire, P. *Fundam. Clin. Pharmacol.* **2008**, *22*, 633–648.